Natural Hazards (2021) 107:575–600
https://doi.org/10.1007/s11069-021-04596-x

ORIGINAL PAPER

Probabilistic seismic hazard assessment studies for Mumbai region

G. Surve[1] · Jyotima Kanaujia[1] · Nitin Sharma[2]

Received: 7 April 2020 / Accepted: 21 January 2021 / Published online: 11 February 2021

Abstract
The present study attempts to understand and assess the seismic hazard of Mumbai using probabilistic seismic hazard analysis (PSHA) with an updated catalogue of earthquake clubbed with recent knowledge on seismotectonics of the region. An updated catalogue of instrumental and pre-instrumental earthquake data within 300 km radius around the city has been compiled from different sources. The PSHA has been computed using two different seismic source models, viz., a fault (linear) and zone model (areal). A hybrid of five suitable ground motion prediction models (GMPM) consisting of widely accepted and latest GMPMs is used to compute the PSHA of Mumbai. The results obtained from different methodologies are integrated with logic tree approach to minimize the epistemic uncertainties in hazard calculation. Probabilistic seismic hazard maps in terms of peak ground accelerations (PGA) at bedrock levels for 2% and 10% probability of exceedance in 50 years are developed for Mumbai. Uniform hazard response spectrum (UHRS) on bedrock at eight different sites within Mumbai for spectral periods of 0.01—2 s is also computed. The low seismic hazard is observed and reasonably compared with the previous PSHA studies done for Mumbai region.

Keywords Peak ground acceleration · Spectral periods · Seismotectonics · Seismic hazard · Logic tree

1 Introduction

The Indian subcontinent has over the years experienced many damaging earthquakes. The main seismogenic zones of India are the north and northeastern parts of the subcontinent and the Andaman & Nicobar Islands which area host to several large earthquakes. The seismicity in these regions is well defined and is primarily due to the inter plate collisions at the boundaries. On the other hand, the southern subcontinent termed as the Peninsular India (PI), wherein the economic capital of India, the city of Mumbai lies, is far away from

✉ G. Surve
ganpat_surve@yahoo.co.in

[1] Indian Institute of Geomagnetism (IIG), Plot No. 5, Sector-18, Near Kalamboli Highway, New Panvel, Navi Mumbai, Maharashtra 410 218, India

[2] CSIR-National Geophysical Research Institute (NGRI), Hyderabad 500007, India

the plate boundaries and is considered as a seismically stable continental region (SCR). Although the seismicity of Peninsular India is presumed to be low to moderate, it has witnessed several devastating intra plate earthquakes in the past few decades, which include Koyna (1967, M_w 6.6), Latur (1993, M_w 6.2), Jabalpur (1997, M_w 5.8) and the recent Bhuj earthquake (M_w 7.7) of January 2001. The frequency of earthquake occurrence is low in such stable continental regions but can cause heavy damage in the affected area and beyond. The main reason behind the damage is the low attenuation of seismic energy with distance in the plate interiors (Hanks and Johnston 1992). Owing to this, even moderate SCR earthquakes can be very destructive. For example, the M_w 6.2, 1993-Latur earthquake caused about 10,000 fatalities (Seeber et al. 1996) and huge damage to property and infrastructure. The most recent, M_w 7.7, Bhuj earthquake of 2001, caused heavy casualties and widespread damage to the buildings and infrastructure in and around the affected region. The effect of the Bhuj earthquake was felt over large distances, as far as Mumbai, which is about 500 km from the earthquake epicenter. The SCR earthquakes are generally rare and occur at shallow focal depths. Their generation mechanism is not yet well understood. However, they usually occur in populated regions which are often unprepared to cope with such a calamity. Hence, the number of fatalities and damage reported from moderate to large earthquakes occurring in such a low strain region is usually significantly higher than their counterparts originating in the tectonic boundary regions. The seismic activity and occurrence of large earthquakes in the SCR are unanticipated as they can be observed clustered around a particular fault for a short time interval and may then migrate to other faults (Crone et al. 1997). Hence, the accuracy in prediction of future large earthquake in the SCR is a difficult and challenging task. Moreover, it is also difficult to identify active seismic faults in the SCR. Quantifying seismic hazard in areas such as the SCR, therefore, poses a big challenge for the researchers. Thus, it is very important to assess the seismic hazard imposed on the major cities situated in such stable continental regions to mitigate the impact of such hazard.

The coastal city of Mumbai is situated on the western coast of the southern Peninsula. Mumbai is the financial capital of India and one of the highly populated cities of the world with a population of over 18 million. The latest seismic hazard zoning map of India (IS1893, 2002) by Bureau of Indian Standards, based on historical records using modified Mercalli intensities (MMI), quantifies the seismic hazard in four levels, zone II-V. As per this seismic zoning map, Mumbai is placed in seismic zone III with a maximum hazard potential of 0.16 g. Over the past four centuries, the city has experienced about 25 earthquakes with intensity IV or greater. Mumbai originally comprised of a cluster of seven islands that over the past two centuries were merged through reclamation of land from the Arabian Sea. These reclaimed regions which constitute a major portion of the city are underlain by soft soil whose properties and thicknesses are unknown. These underlying soft weathered layers of the reclaimed areas may significantly amplify the ground motions due to an earthquake making them highly vulnerable to seismic hazard (Surve and Mohan 2010). The seismotectonic settings together with the socioeconomic importance of the city, makes it imperative to study the seismic hazard potential of the city and the effect of local soil conditions on the ground motion parameter for designing earthquake resistant structures.

The PSHA of any region needs to be revisited or updated by accommodating latest knowledge about the seismotectonics of the region, incorporating improved attenuation relations and taking advantage of the prevailing advance analysis techniques (Frankel 1995). The present work employs the widely adopted method of probabilistic seismic hazard analysis originally proposed by Cornell (1968) to compute the seismic hazard of

Mumbai city. The seismic hazard studies in India date back to the 1960s, when the first seismic zonation map for India was developed by the Bureau of Indian Standards. Several studies adopted the PSHA methodology for evaluating seismic hazard of a region. Iyengar and Ghosh (2004) applied this method for hazard analysis of Delhi. Similarly, Anbazhagan et al. (2009) used this technique to compute seismic hazard of Bangalore city. From engineering perspective, a radius of 300 km around the study area, also termed as the control region, is considered for seismic hazard computation. In this study, the potential seismic sources lying within 300 km radius centered at 19ºN and 72.8ºE are considered for evaluating the hazard for Mumbai city. PSHA is carried out by incorporating latest knowledge about the seismotectonics of the control region along with an updated earthquake catalogue. The spatial variability of seismic hazard for Mumbai is examined using the earthquake catalogue data from 1594 to 2019. A working earthquake catalogue inclusive of instrumental and pre-instrumental data has been compiled for the period 1594–2019 from varied sources**.** It is evident from the spatial distribution of the earthquake catalogue that most of the events are clustered around the Koyna–Warna region (Fig. 1). The seismic hazard of Mumbai has been computed using two different seismic models, linear and areal seismic source models. The linear seismic model identifies 40 faults within the control region, whereas the areal seismic model considers five pre-defined potential seismic zones. Due to the paucity of strong motion data in the peninsular region, only few region-specific GMPEs have been developed. Only two region-specific GMPEs for the PI are available, Raghukanth and Iyengar (2007) and NDMA (2010). The GMPE by Raghukanth and Iyengar (2007) developed specifically for the peninsular India region is used in the present study. In addition, we have used four widely accepted GMPEs developed for similar tectonic regions in the world. A hybrid of these five GMPEs assigning equal weightage to each GMPE is used for hazard analysis. The different set of seismic source models along with the varied GMPEs with suitable weightage is together combined with the logic tree to minimize the uncertainties in the hazard calculations. The peak ground acceleration (PGA) at bedrock level is computed for Mumbai for 2% and 10% probability of exceedance (PE) in 50 years corresponding to return period of 2475 and 475 years, respectively. The PGA values obtained for Mumbai region are found to be lower than the values obtained from previous studies. It is argued that most of the seismic events considered are from the reservoir triggered seismicity from Koyna–Warna region which might have influenced the results obtained in this study.

1.1 Previous seismic hazard studies in Mumbai and Peninsular India

Due to the seismically stable nature of the Peninsular India, very few seismic hazard studies have been carried out for the region. Seismic hazard study based on PSHA for the Indian subcontinent was done by Basu and Nigam (1977) in terms of PGA for a return period of 100 years. A PGA hazard map for India with 10% annual probability of exceedance in 50 years was prepared by Khattri et al. (1984) using the attenuation relation developed by Algermissen and Perkins (1976) for America. Bhatia et al. (1999) prepared a PGA hazard map of India using probabilistic seismic hazard analysis under the Global Seismic Hazard Assessment Program (GSHAP). A detailed PSHA map for Maharashtra was prepared by Seeber et al. (1999). In this study, the region is broadly divided into nine zones based on geology, seismic activity and seismotectonic features. The attenuation relation from Central Eastern United States (CEUS) was used for computing PGA and spectral acceleration (Sa) maps for 500-year return period. The zoneless approach proposed by Frankel (1995)

(a)

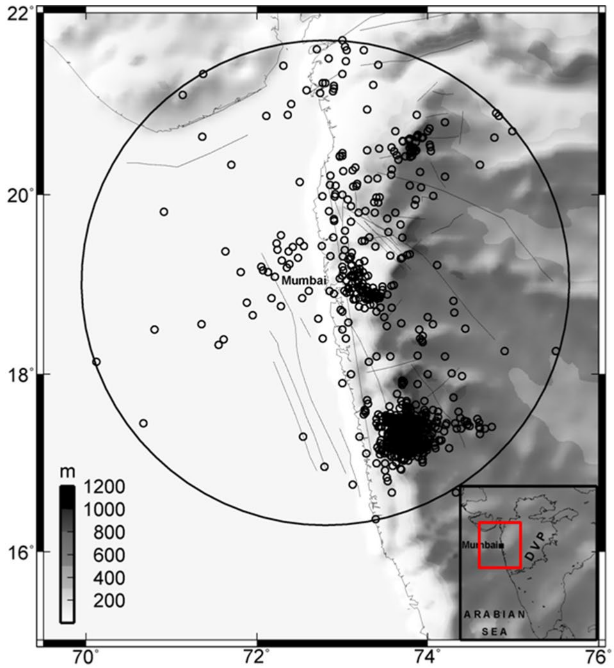

(b)

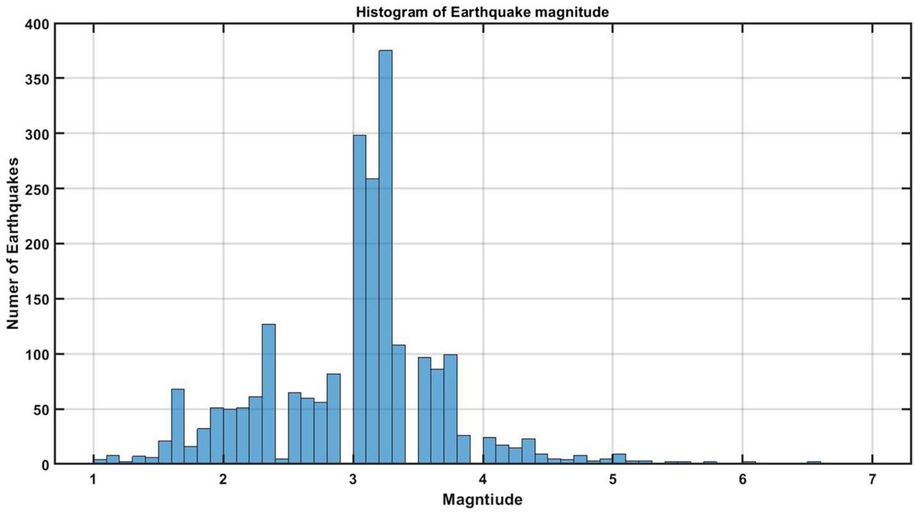

Fig. 1 **a** Topographic map of the study area showing the spatial distribution of earthquakes within a control region of 300 km, centered at 19ºN and 72.8ºE (Mumbai). The forty faults used as linear sources for the study area are also plotted. **b** Histogram of the earthquake catalogue used, showing the distribution of number of events with magnitudes. Inset map depicts the location of study area (in red rectangle) on the Indian Peninsula

was used by Jaiswal and Sinha (2007) for estimating PSHA for peninsular India. Similar approach was used by Nath and Thingbaijam (2012), using the areal sources in a logic tree for computing the PSHA for the Indian subcontinent. An extensive PSHA work, dividing the Indian subcontinent into 32 seismic zones, was carried out by the National Disaster Management Authority of India (NDMA, 2011). Menon et al. (2010) carried out the seismic hazard study for the state of Tamil Nadu.

Raghukanth and Iyengar (2006) derived uniform hazard response spectra (UHRS) for 2% and 10% probability of exceedance in 50 years for different sites in Mumbai. They obtained a recurrence relation for Mumbai using a catalogue of 1274 events from 1594 to 2002 and computed the probability of ground motion induced by each of the 23 faults identified around Mumbai. Vipin et al. (2009) computed the seismic hazard of Mumbai in the PSHA study for the south India region. In both the studies, the estimation of the seismic hazard of Mumbai was done considering point source. Sarika et al. (2014) computed the spatial variability of seismic hazard for Mumbai city, suburbs and adjoining regions of Thane and Navi Mumbai. Sarika et al. (2014) concluded that the seismic hazard for Mumbai and adjoining areas are underestimated in comparison with IS1893:Part1 (2002). However, the most recent seismic hazard study for peninsular India, by Ashish et al. (2016), stated that most of the earlier PSHA studies for Mumbai region delivered higher PGA values. They suggested that the inclusion of Koyna region within the same source zone as Mumbai possibly overestimates the seismic hazard resulting in higher PGA values. The PGA values reported by Ashish et al. (2016) for Mumbai region is 0.067 g at bedrock levels for 10% probability of exceedance in 50 years, which is lower than previous studies.

1.2 Geology and seismotectonics of the study area

The study area falls under the peninsular India that is generally considered as stable continental region (SCR) with low to moderate seismic activity (Chandra, 1977). The control region is characterized by various faults. Subramanyan (2001) has identified active fault lines under the Thane, Panvel and Dharamtor creeks. The N-S trending west coast fault is one of the major prominent faults in the control region whose formation is linked to the breaking of the Indian plate from the Gondwanaland. The other major faults surrounding Mumbai are the Chiplun, Ghod and Warna fault that are secondary manifestations of the west coast fault. The seismicity of this region is intraplate in nature and is understood to be linked with the local faults and weak zones (Rao and Murty, 1970). The study area comprises of the metropolitan city of Mumbai, situated at the west coast of India along the Arabian Sea. It lies in the seismically active Panvel zone (Chandra, 1977), which strikes N-NW along the west coast. The 150-km-long N-S trending Panvel flexure is considered to be active (Nandy, 1995). Recent studies around Mumbai by Mohan et al. (2007) revealed 41 earthquakes of magnitude between M2.5 andM3.5 along the Panvel flexure at crustal depths suggesting the presence of an active fault system beneath it. Seeber et al. (1999) had reported threefold increase in the seismicity of the Peninsular India post 1960. The increase has been attributed to the induced seismicity due to the Koyna dam. The overall seismicity in the control region is diffused, except for few clusters, the prominent one being the Koyna–Warna region. The seismic activity near the Koyna reservoir picked up after its first filling in 1962. It is a classic case of reservoir-induced seismicity. The region witnessed world's largest reservoir induced earthquake (M_w 6.6) on December 10, 1967. The majority of the events in the earthquake catalogue within the control region are due to the reservoir-induced seismicity in the Koyna–Warna region. Gahalaut et al. (2004) argued that the seismicity in the vicinity of the Koyna reservoir may possibly have a contribution from the tectonic component apart from the seismicity triggered due to the water reservoir impoundment. This region is approximately 250 km southeast of Mumbai and can significantly influence the seismic hazard of the city. Owing to the seismic potential of this region, it is considered as a separate seismic zone. The rest of the region within the control region apart from Koyna–Warna is divided in to four zones. The seismicity observed in these four zones is diffused with few clusters of seismicity observed near some of the prominent faults such as the west coast fault, the Panvel flexure, etc. The Panvel flexure is reported to have experienced moderate to large earthquakes in the past.

2 Earthquake catalog

A prerequisite of any seismic hazard analysis is the preparation of an earthquake database for the study area. For the present work, a comprehensive and updated earthquake catalogue for the area within 300 km radius of Mumbai, centered at 19ºN and 72.8ºE, has been compiled for the time interval spanning 1594 to 2019 from different national and international agencies. The instrumental catalogue data published online by various agencies like the National Centre for Seismology (NCS), United States Geological Survey (USGS) & International Seismological Centre (ISC) and available literature were used in the present study. The reviewed version of the ISC earthquake catalogue is used for events from 1964 onwards. The historical earthquakes were compiled from the studies of Chandra (1977), Rao and Rao (1984), and Guha and Basu (1993). Overall, the earthquake catalogue consists of 2260 events for the period 1594 to 2019 (Fig. 1). The composite earthquake catalogue obtained from different sources may have repetitions of some of the large magnitude earthquakes. The duplicate events were identified and removed from the catalogue on the basis of location, time and magnitude of the events. The spatial distribution of the earthquakes along with the potential seismic faults in the control region is shown in Fig. 1. Besides the comprehensive and updated earthquake database, contemporary perspective on the seismotectonics of the region is also reviewed. The Geological Survey of India (GSI) has the compilation of all the data available online (http://bhukosh.gsi.gov.in) for geological, geophysical and seismological features for the entire country. Line sources in terms of active faults and lineaments within the control region were identified and used from this online data. A total of 40 line sources are identified in the study for evaluation of seismic hazard.

2.1 Homogenization of earthquake catalogue

The catalogue compiled from varied sources has events with different magnitude scales that need to be converted to a single magnitude scale for the homogenization of catalogue. Moment magnitude (M_w) is the widely accepted magnitude scale which depends on the fault characteristics. All the magnitude scales in the earthquake catalogue are converted to moment magnitude using the empirical relations proposed by Idriss (1985).

2.2 Declustering of the catalogue

The homogenized catalogue (mainly the instrumental one) contains many dependent events such as foreshocks, aftershocks and clusters of events. The seismicity model requires an earthquake catalogue free of dependent events following the Poisson model of earthquake occurrence. This is accomplished by declustering the earthquake catalogue.

Several algorithms for declustering of raw event catalogues are available (Gardner and Knopoff 1974; Reasenberg, 1985; Molchan and Dmitrieva 1992). In the present study, the Reasenberg (1985) algorithm is used to identify and remove the dependent events from the catalogue. The algorithm assumes that the foreshock and aftershock distribution in space and time are dependent on the magnitude of the primary event. The algorithm removes the events in the space and time window after each causative shock. The declustering procedure is implemented using the Zmap software (Wiemer 2001).

The declustering process identified 147 clusters of earthquakes with 501 events in the study area. The catalogue finally contained 1906 earthquakes after declustering, which was used for further analysis. The declustered catalogue consists of 140 earthquakes with magnitude $M_w \geq 4$ (Fig. 2).

2.3 Completeness of earthquake catalogue

The earthquake catalogues are usually incomplete over the entire magnitude range. This incompleteness in the earthquake database may lead to error in estimation of recurrence rates of earthquakes resulting in overestimation for smaller earthquakes and underestimation for larger earthquakes. Hence, it is essential to check the completeness of the catalogue to minimize these errors and to proceed with further analysis. The completeness analysis computes the magnitude of completeness, M_c, which is the lowest magnitude in the given earthquake catalogue above which all the earthquake magnitudes are recorded in a space–time frame (Rydelek and Sacks, 1989; Woessner and Wiemer 2005). Several methods are available to check the completeness of the catalogue. The two most widely used methods for performing the completeness analysis of earthquake catalogues are the Stepp

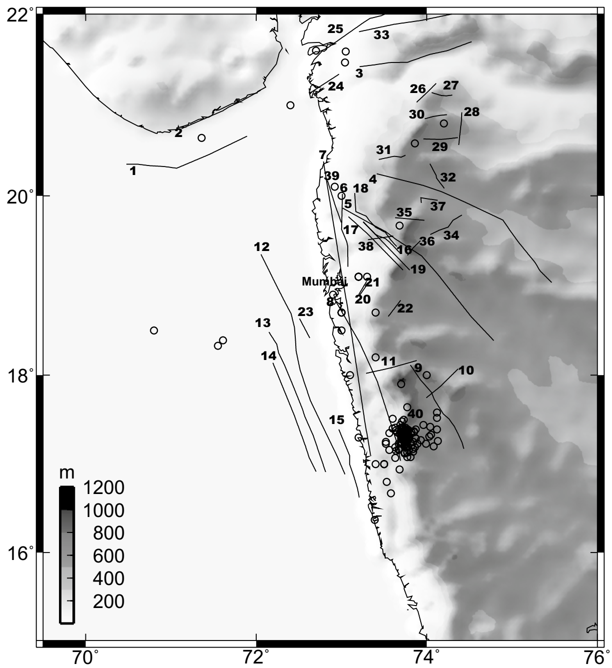

Fig. 2 Topographic map showing the distribution of earthquakes with magnitudes, $M_w \geq 4$ obtained after declustering of catalogue using Raesengberg (1985) declustering algorithm. The forty linear sources (faults) identified and used for seismic hazard analysis are numbered from 1 to 40

(1972) method and the visual cumulative inspection or CUVI method (Tinti and Mulargia 1985). Both these methods are used for completeness analysis. The Stepp (1972) method is a widely used statistical method to calculate the completeness period for different magnitude range of the earthquake catalogue. The CUVI method was employed by Sarika et al. (2014) for Mumbai region and Choudhury and Shukla (2011) utilized this for computing seismic hazard for Gujarat region.

In the CUVI method, two magnitude bin widths of 0.5 and 1.0 units with 10-year time interval are adopted. The entire earthquake catalogue is divided into six different magnitude bins over which that bin can be taken to be complete. Accordingly, the catalogue is grouped into six magnitude bins (Table 1) for computing the period of completeness. The cumulative number of events for each magnitude bin is calculated and plotted against the time period (Fig. 3a). The graph of the cumulative number verses time period is visually checked for the point at which the curve assumes straight line. This point is taken as the period of completeness for the magnitude bins used. The completeness periods for different magnitude bins obtained from the CUVI are summarized in Table 1.

The catalogue completeness is also determined from the Stepp (1972) method for six magnitude classes of 0.5 units magnitude bins, viz., $3.5 \le M_w < 4.0$, $4.0 \le M_w < 4.5$, $4.5 \le M_w < 5.0$, $5.0 \le M_w < 5.5$, $5.5 \le M_w < 6.0$, $6.0 \le M_w$. The average number of earthquakes per year per decade time interval for each magnitude bin is calculated. If for a particular magnitude range the number of events per year is defined as x_1, x_2, ….x_n, then the mean rate per time interval of this sample is given as,

$$\lambda = \frac{1}{n} \sum_{i=1}^{n} x_i \tag{1}$$

where n is number of unit time intervals. The variance is inversely proportional to the length of the sample and defined as,

$$\sigma_\lambda^2 = \frac{\lambda}{T} \tag{2}$$

'T' is the duration of the sample. σ_λ varies as $1/\sqrt{T}$, if λ is considered as a constant. The plot of Stepp method for the six magnitude bins is shown in Fig. 3b, where the standard deviation of the mean rate for the different magnitude bins vs the sample length is plotted. For each magnitude bins, the tangent lines with slope $1/\sqrt{T}$ are plotted. The considered magnitude bin is assumed to be complete up to the point where the plotted data follow a straight line. The results obtained from Stepp and CUVI methods are in close agreement with each other for magnitudes ≥ 4.0.

Table 1 Periods of completeness of earthquake catalogue for different magnitude bins computed using CUVI method

Magnitude interval	Completeness period	No. of years
$3.0 \le Mw < 3.5$	1964–2019	55
$3.5 \le Mw < 4.0$	1954–2019	65
$4.0 \le Mw < 4.5$	1954–2019	65
$4.5 \le Mw < 5.0$	1944–2019	75
$5.0 \le Mw < 6.0$	1924–2019	95
$6.0 \le Mw < 7.0$	1904–2019	115

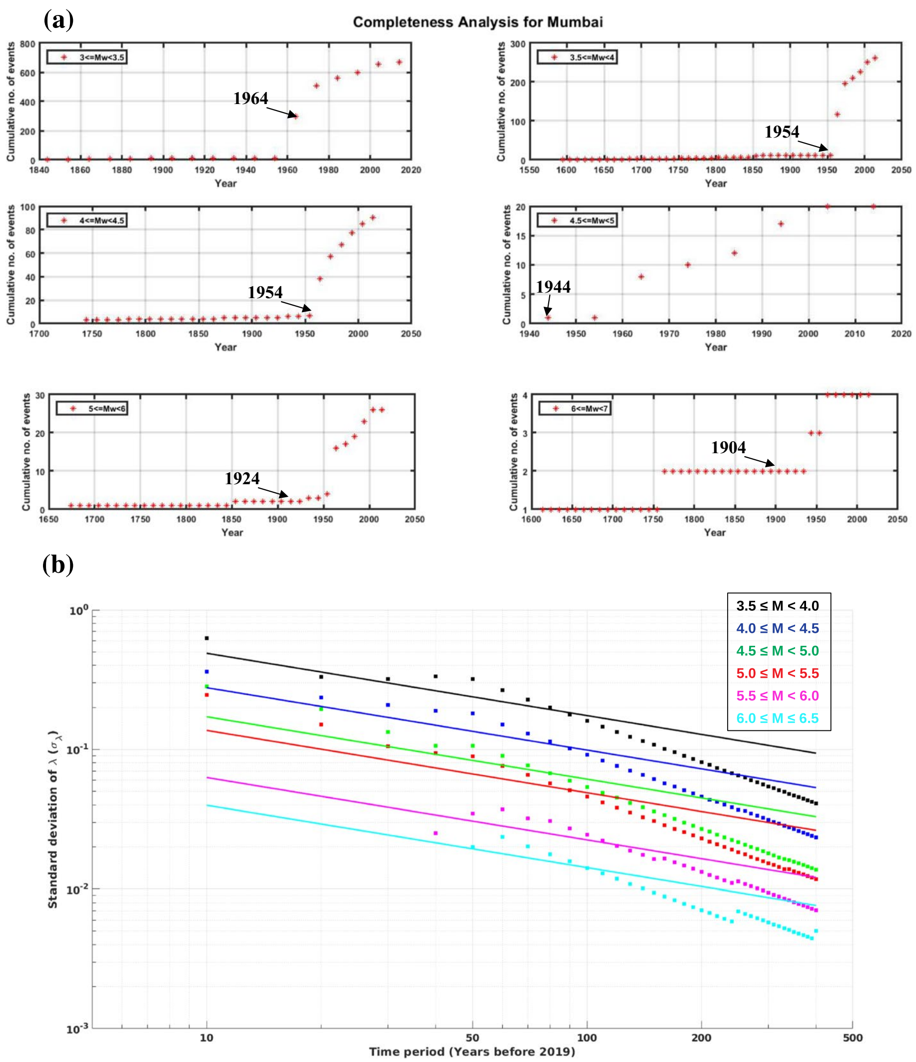

Fig. 3 **a** Plot of completeness analysis performed using visual cumulative inspection or CUVI method (Tinti and Mulargia, 1985) for the earthquake catalogue used in the present study. Completeness analysis is done for different magnitude bins of 0.5 and 1.0 units for six different magnitude intervals ranging from $3.0 \leq M_w \leq 7.0$. The starting year of completeness for a particular magnitude ranges is marked by an arrow. **b** Completeness analysis for the earthquake catalogue using Stepp (1972) method for different magnitude ranges

2.4 Seismicity parameters

The recurrence model parameters define the frequency of earthquakes per year of different magnitudes. The model relates the occurrence of large magnitude earthquakes with respect to the weaker earthquakes. The present study uses the Gutenberg–Richter (GR) magnitude–frequency relationship (1944) to derive the seismicity parameters '*a*' and '*b*'. The values of seismicity parameters ‘*a*’ and ‘*b*’ are estimated using the G–R linear regression relation expressed as below.

$$\log(N) = a - bM_w \; or \, \mathrm{N} = \exp(\alpha - \beta M_w) \tag{3}$$

where N is the number of earthquakes per year with magnitudes equal to or greater than M_w.

a is the background seismicity rate of the region, whereas b value is the slope of the log-linear fit and it represents the magnitude size distribution in the region. α and β are the natural log equivalent of a and b values.

The magnitude of completeness, M_c, and the recurrence parameters have been computed using the Zmap software. Various methods like maximum likelihood, least square and maximum curvature are used to compute M_c. In the present case, the popular method of maximum likelihood (Aki 1965; Utsu 1999) is used to compute the M_c.

The seismicity parameters ‘*a*’ and ‘*b*’ estimated are 3.95 and 0.8008 (Fig. 4), respectively, which are in good agreement with the values obtained by previous researchers (Raghukanth and Iyengar, 2006; Sarika et al., 2014) for Mumbai. The magnitude of completeness, M_c, is computed as 3.0.

2.5 Maximum magnitude

It is the maximum magnitude earthquake expected to occur in the seismic source based on the known seismicity. The Gutenberg–Richter frequency magnitude relation is bounded on the upper end by the maximum magnitude, M_{max} (Knopoff and Kagan 1977). For evaluating M_{max}, the associated fault or zone parameters of the individual sources are a prerequisite. It can be computed by different methods Kijko and Sellevol (1989), the conventional method of increment of 0.5 in the maximum observed magnitude (Nuttli 1979; Gupta 2002a, b), method based on subsurface fault rupture characteristics (Wells and Coppersmith 1994), etc. In the present analysis, two different M_{max} values have been considered, the maximum observed magnitude associated with the seismic source and the other is simply adding 0.5 to this magnitude.

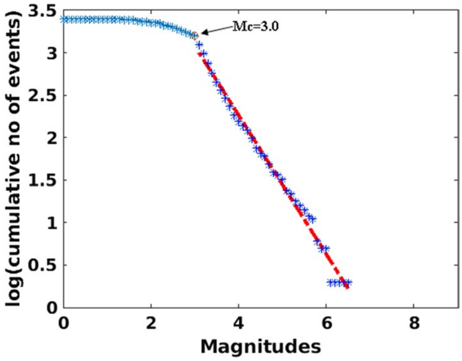

Fig. 4 The Gutenberg–Richter (G–R, 1944) magnitude–frequency relationship for the earthquake catalogue is plotted. The minimum magnitude of completeness estimated is $M_c = 3.0$. Seismicity parameters $a = 3.95$ and $b = 0.8008$ are obtained through regression analysis of G–R relation

3 Seismic source characterization

The most important step in hazard analysis is defining the earthquake sources close to the study area for which seismic hazard is to be quantified. Areas which have experienced earthquakes in the past and are likely be host seismic events in the future are termed as potential seismic sources. The delineation of the potential seismic source zones in the study area is a mammoth task. Range of seismological parameters such as fault mechanism, focal depth, rate of seismicity, tectonics, etc., need to be considered while delineating the seismic sources. These potential seismic sources may be represented in the form of a point, a fault or a region. In the present work, the potential seismic sources are categorized into two different source models, viz., linear source model and the areal source model for evaluation of seismic hazard of Mumbai.

3.1 Linear sources

Seismotectonic and geological features such as faults and lineaments form the linear sources. The Geological Survey of India (GSI) has compiled a comprehensive updated data available online (http://bhukosh.gsi.gov.in) for geological, geophysical and seismological features for the entire Indian region. Active faults and lineaments within the control region are downloaded from this website. A total of 40 line sources (Fig. 1) have been identified and used in the study. In contrast, Raghukanth and Iyengar (2006) used only 23 faults within 300 km radius of Mumbai to compute seismic hazard of the city, whereas Sarika et al. (2014) utilized 31 faults for computing seismic hazard of Mumbai region.

The faults identified in the study region lack information on type of faulting, depth and slip rate. In absence of such fault specific parameters, it is difficult to compute the recurrence relation for individual faults. Hence, the seismicity parameters '*a*' and '*b*' for each fault have been assigned based on regional seismicity parameters. According to the conservation of seismic activity, the overall seismicity rate in a region is equal to the sum of the seismicity rate of individual faults. The same approach has been used by Raghukanth and Iyengar (2006) and Sarika et al. (2014) for computing the seismic hazard for Mumbai region. A weighting factor (η_i) based on the distribution of the catalogue is assigned to the individual faults, where η_i is as follows,

$$\eta_i = \frac{\text{Number of events associated with the source}}{\text{Total number of events in the region}} \tag{4}$$

In addition to the weighting factor (η_i), another weighting factor (μ_i) in terms of length of fault is introduced.

$$\mu_i = \frac{\text{Li}}{\Sigma Li}$$

μ_i is defined as the ratio of individual fault length to the total length of all the faults. The recurrence relation for the i^{th} fault is estimated as below using the average of the two factors.

$$N_i\left(m_0\right) = 0.5\left(\eta_i + \mu_i\right)N(m_0) \tag{5}$$

where $N_i(m_0)$ is the number of earthquakes per year with $m > m_0$ associated with i^{th} fault ($i = 1, 2, 3, \ldots 40$). For seismic hazard computation, m_0, is fixed as 4.0 for all the sources, since earthquakes with magnitudes lower than 4.0 may not cause significant damage to the structures. η_i is the weighting factor in terms of rate of seismicity of the i^{th} fault. It is computed as the ratio of number of earthquakes with magnitude $m \geq 4.0$ attributed to the i^{th} fault to the total number of earthquakes in the region.

Incorporating the weighting factors, the recurrence relation takes the form,

$$N_i(m) = N_i\left(m_0\right)\frac{e^{-(\beta m)} - e^{(-\beta mu)}}{e^{-(\beta m0)} - e^{(-\beta mu)}} m_0 \leq m \leq m_u \quad (6)$$

where m_u is the maximum magnitude of the i^{th} fault and $\beta = 2.303b$. The m_u for each fault is taken as the maximum magnitude event closest to the particular fault. In cases where only a single earthquake lies in close proximity to multiple faults than the same maximum magnitude is allocated to each of these faults. The recurrence relation for the individual fault is truncated in the magnitude range m_o and m_u. The individual weighting factors and the average weighting factors along with the maximum magnitude are reported in Table 2.

3.2 Areal sources

For areal sources, the study area needs to be divided into seismic sources based on seismotectonics of the region. In areal sources, it is assumed that each point within the source has equal probability to be a potential hypocenter of an earthquake. The earthquake occurrence process in the seismic source is independent. The areal source model accounts for unidentified faults in the region under study. In the present study, the potential sources in the study area are broadly categorized into five areal sources (Fig. 5) based on the observed seismicity, geology and the tectonics of the region.

The seismicity of the study area is predominantly governed by the west coast fault (WCF), Chiplun fault (CF) and the Koyna–Warna region. The Koyna–Warna region that is around 250 km southeast of Mumbai city is a classic example of reservoir-induced seismicity worldwide. It has been taken as an independent seismic zone (zone I). The other four zones (zone II—V) encompass the major faults in the region and are categorized accordingly. The seismicity parameters are assigned to the individual seismic zone based on the regional seismicity of the region with appropriate weighting factors similar to that applied in the linear sources as explained in the section above. However, the weighting factor μ_i here is the ratio of the area of the ith individual zone to the total area of all the zones combined, i.e., (Ai/ΣAi). The maximum magnitude for the areal sources is defined based on the spatial distribution of the earthquakes within and around the seismic zone. The earthquake event with maximum magnitude within or nearest to the zone is chosen as the maximum magnitude for that zone. It is observed that some of the faults are seen to overlap in more than one zones (Fig. 4 and 5). For example, the upper Godavari fault (Fault no. 4) lies at the junction of zones III and IV. The west coast fault (WCF) is one of the major faults in the study region which is seismically active and traverses through the zones II to IV. Most of the moderate to large earthquakes in the region are associated with this fault. Although the zones III and IV comprise of faults capable of generating earthquakes with magnitudes within $M \leq 5.0$, the nearest maximum magnitude 5.7 M_w for these zone lies at less than 10 km distances from them. This event is probably associated with the WCF and is and taken as maximum magnitude for both these zones in order to get estimation for maximum damaging earthquake preferably in case of overlapping zones. Likewise for zone V, the magnitude of the nearest large earthquake located west of the zone is taken as the maximum magnitude for zone V. This event is a 1951 historic earthquake whose reported

Table 2 Weighting factors for individual linear seismic source zones used in the present study

Fault no	Fault length (km)	M_{max}	μ_i	η_i	$N_i(m_0)$
1	167	6.0	0.043	0.009	0.0082
2	111	5.5	0.028	0.001	0.0044
3	149	5.0	0.038	0.001	0.0052
4	336	5.0	0.086	0.017	0.0143
5	257	5.0	0.066	0.009	0.0103
6	90	6.5	0.023	0.009	0.0051
7	377	6.5	0.096	0.026	0.0199
8	219	6.5	0.056	0.103	0.0259
9	126	7.0	0.032	0.051	0.0137
10	57	6.0	0.015	0.001	0.0023
11	65	6.0	0.017	0.009	0.0040
12	305	5.5	0.078	0.001	0.0121
13	194	4.5	0.050	0.001	0.0048
14	152	4.5	0.039	0.026	0.0063
15	129	5.5	0.033	0.009	0.0064
16	83	5.5	0.021	0.001	0.0033
17	99	5.5	0.025	0.001	0.0039
18	94	5.5	0.024	0.001	0.0037
19	55	4.5	0.014	0.001	0.0012
20	20	5.0	0.005	0.009	0.0018
21	20	4.5	0.005	0.009	0.0012
22	23	7.0	0.006	0.001	0.0010
23	27	5.5	0.007	0.001	0.0010
24	40	5.0	0.010	0.001	0.0013
25	162	5.0	0.041	0.017	0.0081
26	36	4.5	0.009	0.001	0.0007
27	21	4.5	0.005	0.001	0.0003
28	40	4.5	0.010	0.001	0.0008
29	41	4.5	0.010	0.009	0.0017
30	27	4.5	0.007	0.009	0.0013
31	35	4.5	0.009	0.001	0.0017
32	35	4.5	0.009	0.001	0.0017
33	42	4.5	0.011	0.001	0.0019
34	47	4.5	0.012	0.001	0.0010
35	39	4.5	0.010	0.001	0.0018
36	24	5.0	0.006	0.001	0.0018
37	31	4.5	0.008	0.001	0.0016
38	30	4.5	0.008	0.001	0.0016
39	60	4.0	0.015	0.001	0.0011
40	46	5.0	0.012	0.684	0.0971

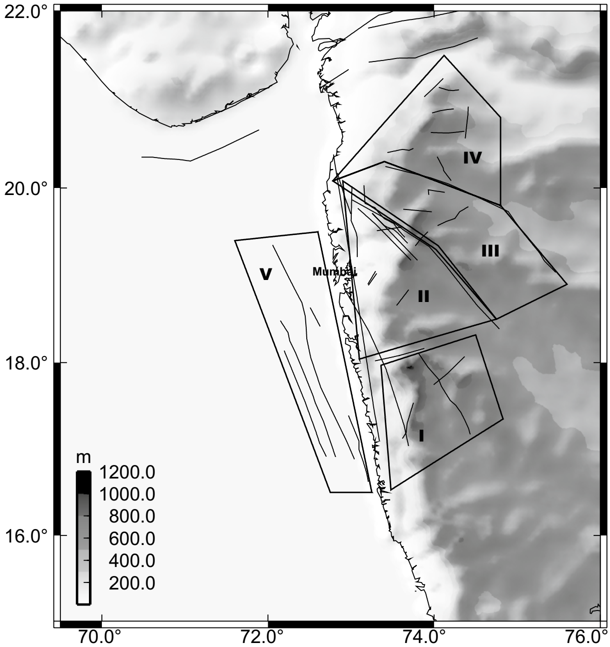

Fig. 5 Topographic map showing the division of five areal seismic sources used for seismic hazard analysis. Areal zones are classified based on the observed seismicity, geology and the tectonics of the region. The zones used as areal sources for present PSHA analysis are numbered as zones I–V

Table 3 Weighting factors for individual areal seismic source zones used in the present study

Zone	Area (Sq. km)	M_{max}	μ_i	η_i	$N_i(mo)$
Koyna_zone	181.14	7.0	0.173	0.911	0.1779
Mum_zone1	216.78	7.0	0.207	0.048	0.0418
Mum_zone2	217.58	6.2	0.207	0.024	0.0375
Mum_zone3	183.46	6.2	0.175	0.016	0.0309
Mum_zone4	250.58	6.5	0.239	0.001	0.039

location is debatable and is therefore considered in zone V for maximum magnitude. The individual weighting factors and the average weighting factors along with the maximum magnitude used for the areal source are reported in Table 3.

4 Ground motion prediction equations

The essential requirement of any seismic hazard analysis is the identification of a suitable ground motion prediction equation (GMPE). The hazard analysis is highly influenced by the choice of GMPE. GMPEs are empirical relations developed based on different earthquake parameters such as the source characteristics, magnitude, fault type, source to site distance, propagation path, etc. It basically relates the ground motion parameters like the peak ground acceleration (PGA) or spectral acceleration (Sa) to the earthquake magnitude, site condition, type of faulting and epicentral distances (Douglas 2003). They are used to compute seismic hazard values at bedrock or ground surface at the site under study for a wide range of time periods. Selection of suitable GMPEs for a region is very essential for seismic hazard study. The seismic hazard analysis has been carried out by various researchers in the Indian subcontinent (Basu and Nigam 1977; Khhatri et al., 1984; Bhatia et al. 1999; NDMA 2011, etc.). The GMPEs used in these studies were developed for similar tectonic settings elsewhere. The GMPE for the peninsular India developed by Raghukanth and Iyengar (2007) is used in the present study. This GMPE was also used by Vipin et al. (2009) and Sarika et al. (2014) for computing PSHA of Mumbai city. The hazard is better represented by combination of GMPEs with the median or mean curve rather than a single curve. In order to overcome the limitations in selection of appropriate GMPEs, those developed for similar tectonic settings worldwide are examined and shortlisted.

The Global Earthquake Model program (GEM 2014) recommends use of GMPEs of Atkinson and Boore (2006), Pezeshk et al. (2011) and Toro (1997) for stable continental regions. The Atkinson and Boore (2006) relation is developed for Eastern North America (ENA) by considering a very large database of events recorded on rock sites. The ground motion attenuation in ENA and peninsular India is comparable (Cramer and Kumar 2003; Bodin et al. 2004), and hence, this relation is used in our study. In the present analysis, the latest and updated relation of Pezeshk (2018) developed for central and eastern North America is also used. A comparison of GMPEs for stable continental regions (Ashish et al., 2016) indicated that use of Toro (1997) yields significantly higher amplitudes. Hence, the relation of Toro (1997) is not used. The widely accepted relations of Abrahamson and Silva (1997) and Campbell (2003) are also used in the present analysis. In all, a hybrid combination of five GMPEs, viz., Abrahamson and Silva (1997), Atkinson and Boore (2006), Campbell (2003), Pezeshk (2018) and Raghukanth and Iyengar (2007), are employed in the present analysis. Table 4 provides the details of the five GMPEs used in the present study. Except for the GMPE by Raghukanth and Iyengar (2007), the other four GMPEs shortlisted for PSHA analysis are GMPEs developed for similar tectonic settings. Although the GMPE for Raghukanth and Iyengar (2007) is developed for PI, it is derived through simulation of synthetic accelerograms and is limited by the point source assumption of seismic source (NDMA 2010). Also, the attenuation relation is valid for epicentral distance range between 30 and 300 km. Hence, it lacks in predicting ground motions from faults in the immediate vicinity of Mumbai (NDMA 2010). Hence, equal weights have been assigned to each of the five GMPEs used in the hybrid form to compute PGA and Sa in the PSHA analysis. Figure 6 depicts the plot of attenuation curves for the five GMPEs along with the hybrid GMPE used in the present PSHA analysis.

5 Logic tree computations and uncertainties

The uncertainties in computation of seismic hazard are broadly classified as aleatory and epistemic uncertainties. The uncertainties in the PSHA calculations because of the randomness in the earthquake occurrence, size and location are termed as aleatory uncertainties. It originates as a result of oversimplification of the otherwise complex modeling processes. The source of epistemic uncertainties or model related uncertainty lies in the lack of sufficient knowledge or fewer input parameters of the models. Epistemic uncertainty can be minimized by incorporating additional data and assigning suitable weights to different input parameters. The uncertainties in the source models used for PSHA calculation need to be taken into account. The epistemic uncertainty is minimized by using the logic tree approach (Kulkarni et al., 1984) in which alternative attenuation models are used by assigning suitable weighting factors. A logic tree is basically characterized by series

Table 4 Details of the five GMPEs used in the present PSHA analysis study

GMPE	Region developed for	Valid Distance range (km)	Spectral period range (sec)	Magnitude range (M_w)
Abrahamson and Silva (1997)—(AS97)	Active shallow crustal tectonic regions	0.1–200	0.01–5.0	4.0–7.5
Atkinson and Boore (2006)—(AB06)	Eastern North America (ENA)	1–1000	0.01–5.0	3.5–8.0
Campbell (2003)—(CA03)	Eastern North America (ENA)	1–1000	0.01–4.0	5.0–8.2
Pezeshk et al. (2018)—(PZ18)	Central and Eastern North America (CENA)	0–400	0.01–10.0	4.0–8.0
Raghukanth and Iyengar (2007)—(RI07)	Peninsular India	30–300	0–4.0	4.0–8.0

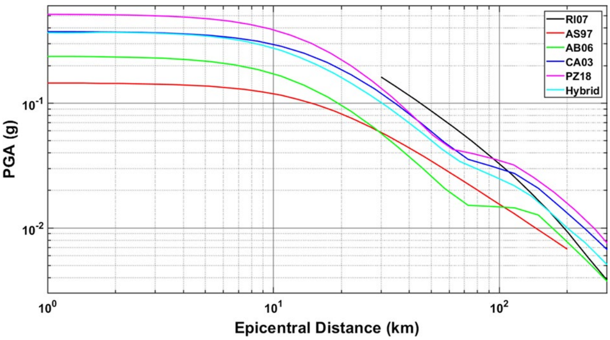

Fig. 6 Plot of attenuation curves showing PGA versus epicentral distance for comparison of five GMPEs used in the present study along with the hybrid GMPE (cyan) formed by assigning equal weights to these five GMPEs

of nodes and branches. Each branch in the logic tree denotes different models which is assigned some pre-defined weight, such that the overall weighting factor at the end branch equals the sum of the weights assigned to individual branches. The sum of all the probabilities at the end of the logic tree should be one.

In the present study, the logic tree with 20 branches is adopted by assigning appropriate weightage to each branch as shown in Fig. 7. The logic tree consists of two seismic source models linear and areal, with two maximum magnitudes and hybrid of five GMPEs.

6 Probabilistic seismic hazard analysis

Seismic hazard computes the ground motion at a given site considering the background seismicity rate, geology, seismotectonics and the attenuation characteristics of the seismic waves in the region. The major application of seismic hazard studies in structural engineering is to develop modern building design codes that are based on seismic parameters derived from statistical analysis of seismicity data. The primary objective of these building codes is to design structures/buildings that can withstand expected ground motion vibrations from earthquakes that it may experience at least once during its lifetime. The commonly used terms in modern building codes are the Design Basis Earthquake (DBE) and Maximum Considered/Credible Earthquake (MCE) (Kramer 1996). DBE is 10% probability of exceedance in 50 years, and MCE is 2% probability of exceedance in 50 years corresponding to return periods of 475 and 2475 years, respectively (Stirling 2014). It is assumed that the expected service life of a typical building is 50 years, hence is generally used as a lifetime for building designs and seismic hazard studies (Stein and Wysession 2003). Seismic hazard studies aim at computing the mean annual rate, i.e., the number of earthquakes per year at a given site thereby estimating the probability of exceedance in the considered lifetime of the structure. The probability of exceedance and lifetime are used to derive the return period that is used to design seismic load of the structure. In the present work, seismic hazard evaluation is done based on PSHA, initially developed by Cornell (1968), and it incorporates the influence of all available potential seismic sources and the associated seismicity rate.

The generalized equation of probabilistic hazard is given as,

$$v_z = \sum_{i=1}^{n} \lambda_i \int_{M_{min}}^{M_{max}} \int_{0}^{r_{max}} f_i(m) f_i(r) P(Z > z|m, r) dr dm \quad (7)$$

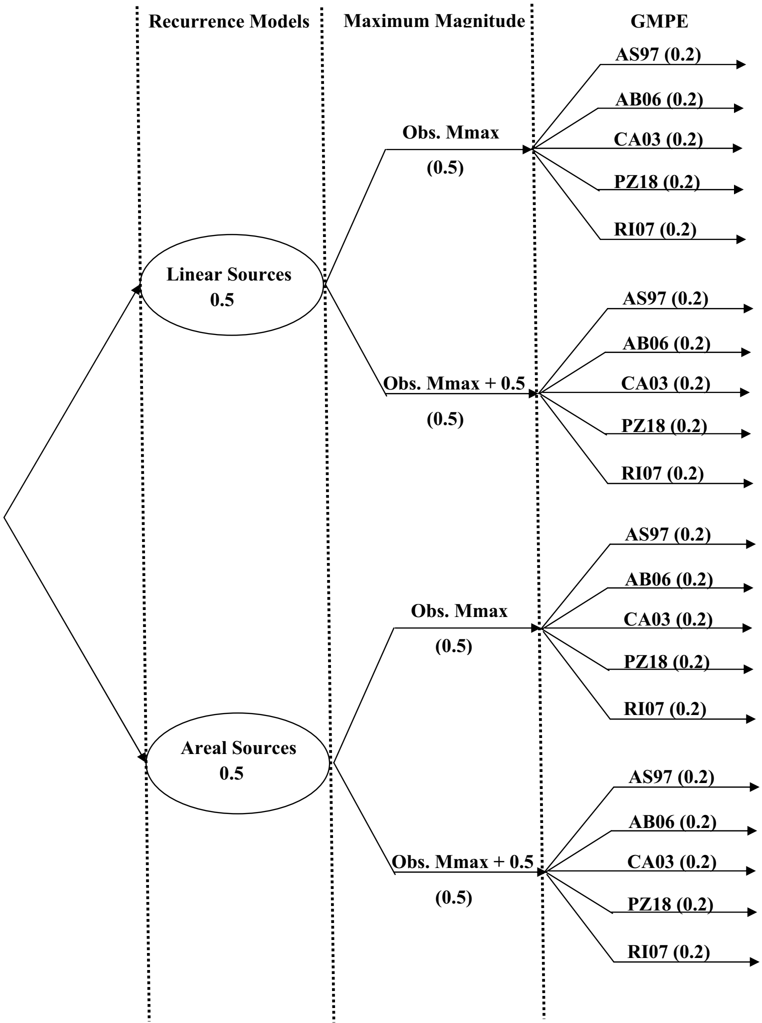

Fig. 7 Logic tree framework showing different branches with different combinations of seismic source models (linear and areal sources), estimated maximum magnitude earthquake (maximum observed magnitude and 0.5 units incremented to the maximum observed magnitude) and GMPEs (five GMPEs) used for computation of seismic hazard in the region. Logic tree consists of 20 branches, wherein each branches are assigned equal weightages

where v_z is the mean annual rate of exceedance of a ground motion level z at a site, λ_i is the mean frequency of occurrence of earthquake exceeding $M_{\min}$ at a source i, $f_i(m)$ and $f_i(r)$ are probability functions of magnitude and distance, respectively, and $P(Z>z|m,r)$ is given by a GMPE. The probability of a certain ground motion, Z, exceeding a certain level z at a site in a time window T years is computed by the following equation.

$$P\left[Z_T > z\right] = 1 - e^{-v_z T} \tag{8}$$

The seismic hazard of Mumbai city is computed using two source models, linear and areal sources. The study done by Cramer and Kumar (2003) concluded that the ground motion attenuation in Eastern North America (ENA) and peninsular India are comparable. Bodin et al. (2004) observed the similarity of regional tectonics of ENA and peninsular India. GMPEs by Atkinson and Boore (2006) developed for the ENA have been used. The computer program R-CRISIS (Ordaz et al. 2017) is used to compute the seismic hazard using both fault and areal source models. The study region is divided into grid size of 0.1°×0.1°, and exceedance rates are obtained for different levels of intensity at 10 spectral ordinates varying between 0.01 and 2 s. A hybrid of five widely accepted GMPEs with equal weight to all is used for computation. The areal source is defined in the program in the form of polygon. The earthquake occurrence process in each zone is assumed to be independent. The minimum and maximum magnitude and associated seismicity parameters are defined for each areal zone. We assumed Poissonian distribution of seismicity for the entire source region. The exceedance probability rates for each seismic source zone are estimated by statistical analysis. The hazard curves in terms of Peak horizontal acceleration (PGA) variation at bed rock level for different time periods are obtained for Mumbai city.

7 Results and discussions

In the present study, an attempt has been made to estimate the seismic hazard of Mumbai city in terms of peak horizontal acceleration (PHA) and spectral acceleration (Sa) at bedrock level based on probabilistic seismic hazard analysis. The study area is divided into grids of size 0.1°×0.1°, and the latest knowledge on seismotectonics of the region is incorporated with updated earthquake catalogue. The earthquake catalogue for the region is compiled for 425 years covering the time interval between 1594 and 2019. All the potential seismic sources within a radius of 300 km are considered for seismic hazard estimates. At each grid point, the peak ground acceleration for 10 different intensities were evaluated at bedrock level for 2% and 10% probability of exceedance in 50 years corresponding to 2475 and 475 years, respectively.

To minimize the associated uncertainties in the attenuation relations, multiple attenuation models are used. The available region-specific attenuation relation developed for peninsular India by Raghukanth and Iyengar (2007) is used in the present study along with four GMPEs accepted worldwide as standard for stable continental regions. These five GMPEs with equal weights are incorporated in hybrid form to evaluate seismic hazard. The seismic hazard is evaluated by considering two seismic source models, linear and areal zones. The hazard computation for both these seismic source models is performed by using the R-CRISIS (Ordaz et al. 2017) software. The uncertainties associated with the hazard computations are minimized by using logic tree framework (Fig. 7). The logic tree developed here primarily consists of two branches of recurrences models 1) linear and 2) areal. Each branch of the recurrence models is further associated with two different approaches of maximum magnitude estimation (i.e., M_{max} and $M_{max}+0.5$). The PHA values are then estimated at each grid point by using the hybrid combination of five GMPEs for each maximum magnitude earthquake, estimated from each seismic source model. The final PHA values obtained are the output of the combination of all 20 branches (which means, different combination of source models, GMPEs and different approaches of M_{max} estimation) of logic tree.

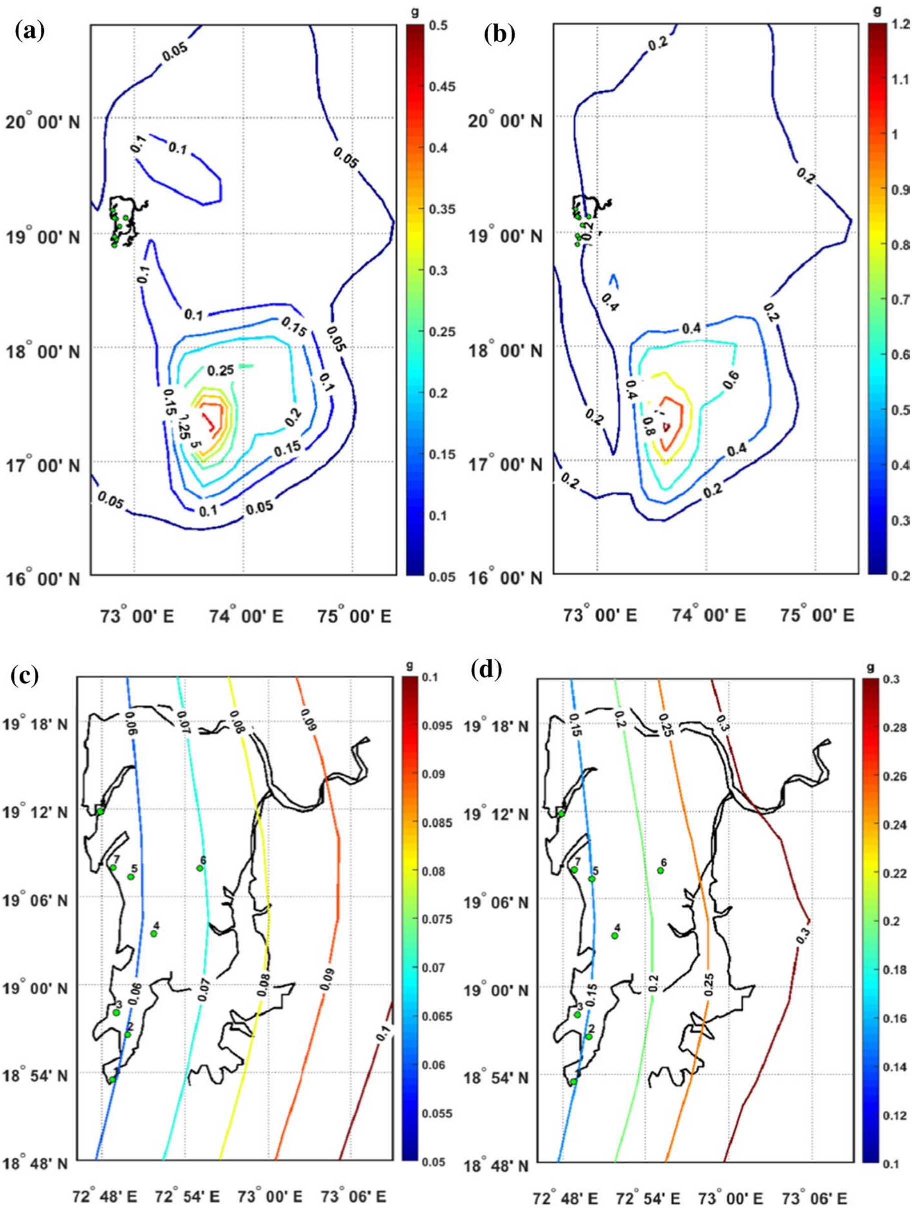

Fig. 8 Contour map of PHA values is obtained using grid spacing of 0.1°×0.1° for the entire study area **a–b** and separately for Mumbai city **c–d** for 475-year and 2475-year return periods corresponds to 10% and 2% of Probability of exceedance (PE) in 50 years, respectively. Maximum PHA value is observed near Koyna–Warna region for both the return periods. The PHA estimates for Mumbai **c** and **d** vary in the range between 0.06 g and 0.09 g for 10% PE in 50 years and between 0.15 g and 0.3 g for 2% PE in 50 years

The spatial variation of peak horizontal acceleration PHA values at bedrock level for Mumbai region corresponding to 10% and 2% probability of exceedance is computed and shown in Fig. 8(a–d). Figure 8(a–d) depicts the PHA values in terms of contours for

Table 5 Peak ground acceleration values (in g) with 10% probability of exceedance in 50 years for Mumbai city compared to previous studies

Previous studies/references	PGA (g)
GSHAP (1999)	0.1
BIS (2002)	0.08
Raghukanth and Iyengar (2006)	0.09
Vipin et al. (2009)	0.1–0.16
NDMA (2011)	0.09
B. Ghosh et. al (2012)	0.047
Sarika et. al (2014)	0.095—0.2
Ashish et. al (2016)	0.067
Present study	0.06–0.09

the entire study area (a–b) and separately for Mumbai city (c–d) for 475-year and 2475-year return periods. As observed from the figure, maximum PHA value is observed near Koyna–Warna region for both 10% and 2% PE of exceedance in 50 years. The PHA estimates for Mumbai (Fig. 8c and d) in the present study vary in the range between 0.06 g and 0.09 g for 10% probability of exceedance in 50 years and between 0.15 g and 0.3 g for 2% probability of exceedance in next 50 years. The peak ground acceleration (PGA) values with 10% probability of exceedance in 50 years at bedrock conditions from previous studies for the city of Mumbai along with the present results are tabulated in Table 5.

Seeber et al. (1999) estimated the PHA values for Mumbai region, specific to B-C sites, for 2% and 10% probability of exceedance in 50 years as 0.33 g and 0.15 g, respectively. The bedrock values for Mumbai as reported by Bhatia et al. (1999) under the Global Seismic Hazard Assessment Program (GSHAP) is 0.1 g. Raghukanth and Iyengar (2006) exclusively carried out PSHA studies for Mumbai city and estimated the bedrock PHA values of 0.09 g and 0.18 g, respectively, for return periods of 475 and 2475 years (Table 5). A similar study for computing seismic hazard for 475-year and 2475-year return periods for Mumbai region involving Mumbai city, suburbs and part of Thane and Navi Mumbai is done by Sarika et al. (2014). They obtained PHA values for Mumbai region in the range of 0.095—0.2 g for 475-year return period and 0.17—0.37 for 2475-year return period. Their results indicated that the adjoining regions of Thane and Navi Mumbai are expected to have higher seismic potential compared to the city of Mumbai and its suburbs for both the return periods. The PHA values for Mumbai as per the IS 1893: Part I (2002) are, respectively, 0.08 g and 0.16 g for 475-year and 2475-year return periods. Vipin et al. (2009) computed seismic hazard study in terms of PHA, spectral acceleration and UHRS at bedrock levels for south India and estimated the PHA values for Mumbai city in the range of 0.1 g to 0.16 g for 475 years and 0.15 to 0.3 g for 2475-year return period. They also estimated the PGA at ground surface levels for South India in different site classes A to D based on average shear wave velocity in the top 30 m (v_s^{30}). The National Disaster Management Authority (NDMA, 2011) developed comprehensive PSHA maps for the entire Indian region. It provides PHA values for important cities of India. NDMA (2011) estimated a value of 0.09 g corresponding to 475-year return period for city of Mumbai. The PHA levels obtained in the present study for Mumbai are slightly on the lower side as compared to the values estimated from most of the previous studies discussed herein (Table 5). However, some of the recent studies, e.g., Ghosh et al. (2012), Ashish et al. (2016), etc., have reported values of 0.047 g and 0.067 g, respectively, for 10% PE in 50 years for Mumbai, which are comparable to the values obtained in the present study.

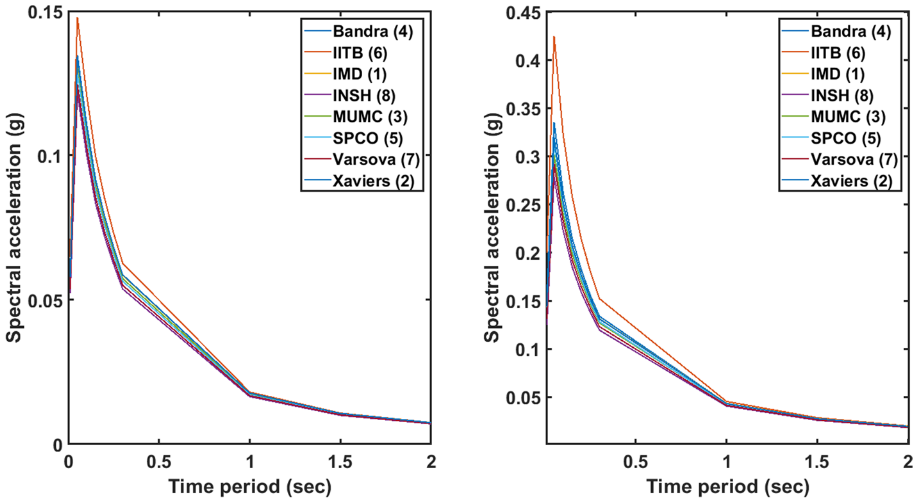

Fig. 9 Uniform Hazard Response Spectra (UHRS) for ten spectral periods between 0.01 and 2 s is computed for 8 different sites within Mumbai for 10% (left) and 2% (right) PE in 50 years. A maximum PHA of around 0.15 g and ~ 0.43 g for 10% and 2% probability of exceedance in 50 years, respectively, is observed in the UHRS plot

The peak ground acceleration values are normally used to characterize the ground motion; however for design of engineering structures, the spectral acceleration (Sa) is generally preferred. The spectral acceleration is represented by the uniform hazard response spectrum (UHRS). The UHRS provides acceleration values at different spectral periods, which are very much useful to the civil engineers for designing structures. In the present study, the spectral acceleration values for bedrock levels at ten spectral periods varying between 0.01 and 2 s are obtained. The UHRS at bedrock levels for return periods of 475 and 2475 years at eight different sites (shown in Fig. 8c) selected randomly within Mumbai is computed (Fig. 9). The UHRS values obtained at the eight sites within Mumbai have a maximum of around 0.15 g and approximately 0.43 g for 10% and 2% probability of exceedance in 50 years.

The Sa values estimated for 1 sec period in the present analysis range between 0.016 g and 0.018 g and 0.04 g to 0.045 g for 475-year and 2475-year return periods, respectively. The Sa values at 1 sec reported by Vipin et al. (2009) for return periods of 475 and 2475 years are, respectively, in the range 0.04 g to 0.06 g and 0.04 to 0.08 g. These values computed for 10% probability of exceedance in 50 years are less when compared with previous studies.

7.1 Interpretation of the results

The lower seismic hazard values can be attributed to the fact that in this study, Koyna–Warna region is considered as one of the five independent source regions. According to the recent study carried by Kao et al. (2018) and the arguments presented by Barbour and Pollitz (2019), it is inferred that the induced seismicity can plausibly result in overall reduction of seismic hazard estimation. The anthropogenic activities like fluid injection, waste-fluid disposal and hydraulic cracking, etc., increase the number of earthquakes. The remarkable increase in number of earthquakes can actually cause change in overall seismic hazard estimations. It is expected that the accumulated strain in upper crustal level is released through occurrence of small magnitude-induced earthquakes which ultimately avoids the occurrence of large magnitude earthquake.

The seismicity in and around Koyna–Warna region is very well established as reservoir-induced seismicity (Gupta et al. 1992, 2002,2005). The seismicity in this zone has increased after the construction of the Koyna dam and has persisted for more than six decades. The region has experienced about 22 earthquakes of M > 5, nearly 200 earthquakes of M ~ 4 and thousands of smaller earthquakes since 1962, following impoundments of Koyna reservoir in 1961 and Warna reservoir in 1985 (Dixit et al., 2014). The seismicity induced due to the impoundment of reservoir might have resulted in release of accumulated strain through several small magnitude earthquakes, thereby resulting in overall reduction in PHA estimations, as also argued by Kao et al. (2018) and Barbour and Pollitz (2019).

8 Conclusion

The present study evaluates the seismic hazard at Mumbai using the probabilistic seismic hazard analysis. Two seismicity models, linear and areal, are used to compute seismic hazard of Mumbai with updated earthquake catalogue and applying latest knowledge on seismotectonics of the region. Forty potentially active seismic faults and lineaments that can trigger ground motion at Mumbai have been identified within the 300 km radius centered at Mumbai. In the areal seismicity model, the potential seismic sources were divided into five seismic zones. The PHA values for Mumbai corresponding to 475-year and 2475-year return periods are computed. The uniform hazard spectra for the two return periods are also derived. Many of the earlier studies for the study area have utilized only a single attenuation relation (Bhatia et al. 1999; Vipin et al. 2009). The present study utilizes a set of GMPEs in hybrid form with two different recurrence models linear and areal combined into one with the logic tree approach. The hazard maps at bedrock level for 2% and 10% probability of exceedance in 50 years are prepared for Mumbai. The PHA values obtained in the present study are lower than those reported for the same area by previous researchers. The lower seismic hazard can be attributed to the facts that in this study, Koyna–Warna region is used as one of the five independent source regions and reservoir triggered seismicity at times might reduce the overall seismic hazard in nearby regions. Thus, the obtained overall PHA in this study is lower than those from past studies. The adoption of above-mentioned technique affirms that the results presented in the study are realistic and will be useful for identifying potential hazard conditions for Mumbai region.

Acknowledgements GS and JK are thankful to the Director, Indian Institute of Geomagnetism, Navi Mumbai, for providing valuable suggestions, guidance and kind permission to publish this work. This work is a part of the GS's Ph.D research work. GS is thankful to his Ph.D supervisors, Prof. D. S. Ramesh, Director, IIG, Navi Mumbai and Prof. K. Vijaya Kumar, Director, School of Earth Sciences, Swami Ramanand Teerth Marathwada University, Nanded, for their continued guidance, motivation and support for carrying out the research work. JK is thankful to the NMRF research grant, IIG to support her research work. NS is thankful to the support and grant received from Earthquake Hazard Studies Group under the project MLP-6401-28 (DSN) of CSIR—National Geophysical Research Institute, Hyderabad. The authors gratefully acknowledge the two anonymous reviewers for their detailed and critical review with constructive comments that significantly improved the article. The authors thank the Editor-in-Chief, Prof. Harsh K. Gupta, for valuable suggestions.

Data availability Earthquake catalogue used in this study was compiled using data available online from various agencies such as National Center for Seismology (NCS), India (https://seismo.gov.in/content/seismological-bulletins), United States Geological Survey (USGS) https://earthquake.usgs.gov/earthquakes/search/ & International Seismological Centre (ISC) http://www.isc.ac.uk/iscbulletin/search/catalogue/.

Compliance with ethical standards

Conflict of interest The authors declare that they have no conflict of interest.

References

Abrahamson NA, Silva WJ (1997) Empirical response spectral attenuation relations for shallow crustal earthquakes. Seismol Res Lett 68(1):94–127
Aki K (1965) Maximum likelihood estimate of b in the formula log N = a-bm and its confidence limits. Bull Earthq Res Inst Univ Tokyo 43:237–239
Algermissen ST, Perkins DM (1976) A probabilistic estimate of maximum acceleration in rock in the contiguous United States. USGS Open File Rep 76:45
Anbazhagan P, Vinod JS, Sitharam TG (2009) Probabilistic seismic hazard analysis for Bangalore. Nat Hazards 48:145–166
Ashish Lindholm C, Parvez IA, Kuhn D (2016) Probabilistic earthquake hazard assessment for peninsular India. J Seismol 20(2):629–653
Atkinson GM, Boore DM (2006) Earthquake ground-motion predictions for eastern North America. Bull Seismol Soc Am 96:2181–2205
Barbour AJ, Pollitz F (2019) Induced seismicity reduces seismic hazard? Geophys Res Lett 46:4170–4173. https://doi.org/10.1029/2019GL081991
Basu S, Nigam NC (1977) Seismic risk analysis of Indian peninsula. In Proceedings of Sixth World Conference on Earthquake Engineering, New Delhi. Vol. I: 782–788
Bhatia SC, Kumar MR, Gupta HK (1999) A probabilistic seismic hazard map of India and adjoining regions. Ann Geofis 42:1153–1166
Bodin P, Malagnini L, Akinci A (2004) Ground motion scaling in the Kachchh basin, India, deduced from the aftershocks of the 2001 Mw 7.6 Bhuj earthquake. Bull Seismol Soc Am 94:1658–1669
Bureau of Indian Standards (BIS) (2002) IS 1893–2002 (Part 1): Indian standard criteria for earthquake resistant design of structures, Part 1–general provisions and buildings. Bureau of Indian Standards, New Delhi
Campbell KW (2003) Prediction of strong ground motion using the hybrid empirical method and its use in the development of ground motion (attenuation) relations in eastern North America. Bull Seism Soc Am 93:1012–1033
Chandra U (1977) Earthquakes of peninsular India – a seismotectonic study. Bull Seism Soc Am 67:1387–1413
Choudhury D, Shukla J (2011) Probability of occurrence and study of earthquake recurrence models for Gujarat state in India. Disaster Adv 4(2):47–59
Cornell CA (1968) Engineering seismic risk analysis. Bull Seism Soc Am 58:1583–1606
Cramer CH, Kumar A (2003) 2001 Bhuj, India, earthquake engineering seismoscope recordings and eastern North America ground motion attenuation relations. Bull Seism Soc Am 93:1390–1394
Crone AJ, Machette MN, Bowman JR (1997) Episodic nature of earthquake activity in stable continental regions revealed by paleoseismicity studies of Australian and North American Quaternary faults. Aust J Earth Sci 44:203–214
Dixit MM, Kumar S, Catchings RD, Suman K, Sarkar D, Sen MK (2014) Seismicity, faulting, and structure of the Koyna-Warna seismic region, western India, from local earthquake tomography and hypocenter locations. J Geophys Res Solid Earth 119:6372–6398. https://doi.org/10.1002/2014JB010950
Douglas J (2003) Earthquake ground motion estimation using strong-motion records: a review of equations for the estimation of peak ground acceleration and response spectral ordinates. J Earth-Sci Rev 61:43–104
Desai SS, Choudhury D (2014) Spatial variation of probabilistic seismic hazard for Mumbai and surrounding region. Nat Hazards 71:1873–1898
Frankel A (1995) Mapping seismic hazard in the Central Eastern United States. Seism Res Lett 66(4):8–21

Gahalaut VK, Kalpana VK, Singh SK (2004) Fault interaction and earthquake triggering in the Koyna-Warna region. India Geophys Res Lett 31(11):1–4
Gardner JK, Knopoff L (1974) Is the sequence of earthquakes in southern California, with aftershocks removed, Poissonian? Seism Soc Am 64:1633–1638
Geological Survey of India, http://bhukosh.gsi.gov.in
Ghosh B, Pappin JW, So MML, Hicyilmaz KMO (2012) Seismic hazard assessment in India. In 15th world conference on earthquake engineering http://www.iitk.ac.in/nicee/wcee/article/WCEE2012_2107.pdf
Global Earthquake Model (GEM 2014) http://www.globalearthquakemodel.org
Guha SK, Basu PC (1993) Catalogue of earthquake (M≥3) in Peninsular India. Atomic energy regulatory board, Tech document no. TD/CES-1, 1–70
Gupta ID (2002a) The state of the art in seismic hazard analysis. ISET J Earthq Technol 39(4):311–346
Gupta HK (1992) Reservoir-induced earthquakes. Elsevier, Amsterdam
Gupta HK (2002b) A review of recent studies of triggered earthquakes by artificial water reservoirs with special emphasis on earthquakes in Koyna, India. Earth Sci Rev 58:279–310
Gupta HK (2005) Artificial water reservoir-triggered earthquakes with special emphasis at Koyna. Curr Sci 88(10):1628–1631
Gutenberg B, Richter CF (1944) Frequency of earthquakes in California. Bull Seism Soc Am 34:185–188
Hanks TC, Johnston AC (1992) Common features of the excitation and propagation of strong ground motion for North American earthquakes. Bull Seismol Soc Am 82(1):1–23
Idriss IM (1985) Evaluating seismic risk in engineering practice. Proceedings of the 11th Intl Conference on Soil Mechanics and Foundation Engineering. San Francisco 1: 255–320
Iyengar RN, Ghosh S (2004) Microzonation of earthquake hazard in greater Delhi area. Curr Sci 87:1193–1202
Jaiswal K, Sinha R (2007) Probabilistic seismic-hazard estimation for peninsular India. Bull Seism Soc Am 97:318–330
Kanth STGR, Iyengar RN (2006) Seismic hazard estimation for Mumbai city. Curr Sci 91:1486–1494
Kao H, Hyndman R, Jiang Y, Visser R, Smith B, Babaie Mahani A et al (2018) Induced seismicity in western Canada linked to tectonic strain rate: implications for regional seismic hazard. Geo Res Lett 45:11104–11115. https://doi.org/10.1029/2018GL079288
Khattri KN, Rogers AM, Perkins DM, Algermissen ST (1984) A seismic hazard map of India and adjacent areas. Tectonophysics 108:93–134
Kijko A, Sellevoll MA (1989) Estimation of earthquake hazard parameters from incomplete data files. Part I Bull Seismol Soc Am 79:645–654
Knopoff L, Kagan Y (1977) Analysis of the theory of extremes as applied to earthquake problems. J Geophys Res 82:5647–5657
Kramer SL (1996) Geotechnical earthquake engineering. Prentice-Hall international series in Civil Engineering and Engineering Mechanics. Prentice-Hall, New Jersey
Kulkarni RB, Youngs RR, Coppersmith KJ (1984) Assessment of confidence intervals for results of seismic hazard analysis. In Proceedings, Eighth World Conference on Earthquake Engineering, San Francisco, 263–270
Menon A, Ornthammarath T, Corigliano M, Lai CG (2010) Probabilistic seismic hazard macrozonation of Tamil Nadu in southern India. Bull Seism Soc Am 100(1):320–341
Mohan G, Surve G, Tiwari P (2007) Seismic evidences of faulting beneath the Panvel flexure. Current Sci 93:991–996
Molchan G, Dmitrieva O (1992) Aftershock identification: methods and new approaches. Geophys J Int 109:501–516
Nandy DR (1995) Neotectonism and seismic hazards in India. Indian J Geol 67:34–48
Nath SK, Thingbaijam KKS (2012) Probabilistic seismic hazard assessment of India. Seismol Res Lett. https://doi.org/10.1785/gssrl.83.1.135
National Disaster Management Authority (NDMA) (2010) Development of probabilistic seismic hazard map of India technical report by National Disaster Management Authority. Government of India, Delhi
National Disaster Management Authority (NDMA) (2011) Development of Probabilistic Seismic Hazard Map of India. Govt of India
Nuttli OW (1979) Seismicity of the central United States. Geological Society of America. Rev Eng Geol 4:67–93
Ordaz M, Martinelli F, Aguilar A, Arboleda J, Meletti C, D'Amico V (2017) R-CRISIS Program and platform for computing seismic hazard

Pezeshk S, Zandieh A, Tavakoli B (2011) Hybrid empirical ground-motion prediction equations for Eastern North America using NGA models and updated seismological parameters. Bull Seism Soc Am 101(4):1859–1870. https://doi.org/10.1785/0120100144

Pezeshk S, Zandieh A, Campbell KW, Tavakoli B (2018) Ground-motion prediction equations for Central and Eastern North America using the hybrid empirical method and NGA-West2 empirical ground-motion models. Bull Seismol Soc Am 108(4):2278–2304

Raghukanth STG, Iyengar RN (2007) Estimation of seismic spectral acceleration in peninsular India. J Earth Syst Sci 116:199–214

Rao BV, Murty BVS (1970) Earthquakes and tectonics in peninsular India. J Indian Geophys Union 7:1–9

Rao BR, Rao PS (1984) Historical seismicity of peninsular India. Bull Seism Soc Am 74:2519–2533

Reasenberg P (1985) Second-order moment of central California seismicity 1969–1982. J Geophys Res 90:5479–5495

Rydelek PA, Sacks I (1989) Testing the completeness of earthquake catalogues and the hypothesis of self similarity. Nature 337:251–253

Seeber L, Ekstrom G, Jain SK, Murty CVR, Chandak N, Armbruster JG (1996) The 1993 Killari earthquake in central India: a new fault in Mesozoic basalt flows. J Geophys Res 101:8643–8560

Seeber L, Armbruster JG, Jacob KH (1999) Probabilistic assessment of earthquake hazard for the state of Maharashtra. Unpublished Report. Government of Maharashtra, Earthquake Rehabilitation Cell, Mumbai

Stein S, Wysession M (2003) An introduction to seismology, earthquakes, and earth structure. Blackwell Pub, Malden, MA

Stepp JC (1972) Analysis of completeness of the earthquake sample in the Puget sound area and its effect on statistical estimates of earthquake hazard. Int Conf Microzonat II:897–909

Stirling M (2014) The Continued Utility of Probabilistic Seismic-Hazard Assessment: p. 359–376.

Subrahmanyan V (2001) Seismic signatures in the Kalu River Basin, Thane district and Mumbai, in: Research Highlights in Earth System Science. Indian Geological Congress 201–204

Surve G, Mohan G (2010) Site response studies in Mumbai using (H/V) Nakamura technique. Nat Hazards 54:783–795

Tinti S, Mulargia F (1985) Completeness analysis of a seismic catalog. Ann Geophys 3:407–414

Toro GN (1997) Model of strong ground motion in eastern and central North America: best estimates and uncertainties. Seismol Res Lett 68:41–57

Utsu T (1999) Representation and analysis of the earthquake size distribution: a historical review and some new approaches. Pure Appl Geophys 155:509–535

Vipin KS, Anbazhagan P, Sitharam TG (2009) Estimation of peak ground acceleration and spectral acceleration for south India with local site effects: probabilistic approach. Nat Hazards 9:865–878

Wells DL, Coppersmith KJ (1994) Updated empirical relationships among magnitude, rupture length, rupture area and surface displacement. Bull Seismol Soc Am 84:4–43

Wiemer S (2001) A software package to analyze seismicity: zmap. Seismol Res Lett 72(2):374–383

Woessner J, Wiemer S (2005) Assessing the quality of earthquake catalogue: estimating the magnitude of completeness and its uncertainty. Bull Seismol Soc Am 95(2):684–698